

# SENSITIVITY AND UNCERTAINTY ANALYSIS OF FUEL PERFORMANCE ASSESSMENT OF CHROMIA-DOPED FUEL DURING LARGE-BREAK LOCA

YIFENG CHE, XU WU, WEI Li, KOROUGH SHIRVAN\*

*Department of Nuclear Science and Engineering, Massachusetts Institute of Technology  
Cambridge, Massachusetts, 02139, USA*

*\*Email: [kshirvan@mit.edu](mailto:kshirvan@mit.edu)*

GIOVANNI PASTORE, JASON HALES

*Fuel Modeling and Simulation Department, Idaho National Laboratory  
Idaho Falls, Idaho, 83402, USA*

## ABSTRACT

Cr<sub>2</sub>O<sub>3</sub>-doped UO<sub>2</sub> fuel is a promising near-term accident tolerant fuel (ATF) candidate due to its enhanced fission gas retention and improved pellet-cladding mechanical interaction (PCMI) behavior. The enhanced accident tolerance of Cr<sub>2</sub>O<sub>3</sub>-doped UO<sub>2</sub> fuel is illustrated through the modeling of a Large-Break Loss-of-Coolant Accident (LB-LOCA) case. A sensitivity analysis (SA) is performed based on the LB-LOCA case in DAKOTA using the Morris screening method. The number of uncertain BISON input parameters is reduced based on the SA result, providing a limited set of parameters that significantly impact the figure of merits (FOMs). The uncertainties in the FOMs are then quantified by propagating the uncertainties in the significant parameters using Latin Hypercube Sampling. It is found that Cr<sub>2</sub>O<sub>3</sub>-doped UO<sub>2</sub> fuel has an improved fuel performance within the uncertainty in the predictions.

**Keywords:** Chromia-doped Fuel; Fuel Performance Modeling; Large Break LOCA; Sensitivity Analysis; Uncertainty Quantification

## 1 Introduction

While accident tolerant fuels (ATFs) focus on improving the accident tolerance of nuclear reactors, they must also exhibit superior operational reliability and flexibility during anticipated operation occurrences (AOOs) and Design-Basis-Accidents (DBAs) in order to justify the cost of their development. Improved operational fuel performance can arise from delayed and reduced fission gas release and improved pellet-cladding mechanical interaction (PCMI), which can potentially delay the ballooning or burst of the cladding upon accidents [1]. Cr<sub>2</sub>O<sub>3</sub>-doped UO<sub>2</sub> fuel is one of the most promising near-term ATF candidates that could exhibit such improvements. Small amount of Cr<sub>2</sub>O<sub>3</sub> additives can serve as effective grain growth promoter, increasing the average fuel grain size up to 5-7 times larger compared to the standard UO<sub>2</sub> fuel [2][3][4]. Larger grain size increases the diffusion path for the gaseous fission products, delaying the onset of fission gas release and enhancing the fission gas retention [1]. To achieve enlarged grain size, lower sintering temperature and shorter sintering times are required in the Cr<sub>2</sub>O<sub>3</sub>-doped UO<sub>2</sub> compared to the undoped UO<sub>2</sub>, reducing the manufacturing cost and economic penalty [5]. In addition to the enhanced fission gas retention, Cr<sub>2</sub>O<sub>3</sub>-doped UO<sub>2</sub> fuel exhibits more numerous but smaller cracks at the pellet rim during the

reactor operation, which is beneficial from the perspective of PCMI [6]. The enhanced fission gas retention and PCMI jointly make the Cr<sub>2</sub>O<sub>3</sub>-doped UO<sub>2</sub> fuel more accident tolerant.

Uncertainties in fuel performance modeling might arise from fuel manufacturing, reactor operation and simplified underlying physical models. For this reason, it is important to demonstrate the response uncertainties in order for regulators to make sound decision concerning public safety [7]. The uncertainty propagation in fuel performance modeling is challenging due to the sophisticated and coupled thermal-mechanical processes. Performing Sensitivity Analysis (SA) preceding the Uncertainty Quantification (UQ) can provide an idea of how much each uncertain parameter contributes to the overall uncertainty, as well as an efficient way of dimensional reduction. Uncertainty quantification based on reasonably filtered uncertain inputs requires less computational resources, while at the same time it can provide satisfying estimation of the uncertainty. In this work, the performance of UO<sub>2</sub> fuel and Cr<sub>2</sub>O<sub>3</sub>-doped UO<sub>2</sub> fuel is modeled under a Large Break LOCA (LB-LOCA) scenario using the fuel performance code BISON [8]. A full list of BISON input parameters and their corresponding uncertain ranges are presented. SA is carried out using the Morris Screening method regarding selected figure of merits (FOM), and the uncertain inputs are screened based on the SA result. UQ is subsequently performed with respect to the same FOMs using Latin Hypercube Sampling (LHS).

## 2 Morris Screening for Sensitivity Analysis

Morris screening [9] is used in this work for sensitivity study, which can rank the importance of the model parameters using a relatively small number of computer model evaluations. Morris elementary effects method [10], also called Morris One-At-A-Time (MOAT), is the global extension of the one-at-a-time (OAT) method. With OAT method, model input parameters are varied one at a time while keeping the others fixed. MOAT performs computer experiments that consist of individually randomized designs which vary one input at a time to create a sample of its elementary effects (EE). Given a model  $y(\mathbf{x})$  where  $\mathbf{x} = [x_1, x_2, \dots, x_K]$  is the  $K$ -dimensional input vector, the EE corresponds to  $i^{\text{th}}$  input at the  $n^{\text{th}}$  reference point is defined as:

$$EE_i^n = \frac{y(\mathbf{x}^n + \Delta_i) - y(\mathbf{x}^n)}{\Delta_i}$$

where  $\Delta_i$  is the grid jump in the  $i^{\text{th}}$  dimension. In contrast to the traditional OAT method, MOAT samples the EEs for each input  $N$  times while randomly select the reference point  $\mathbf{x}^n$  from the whole input space. Define the mean, modified mean and standard deviation of the EEs for each input parameter as:

$$\mu_i = \frac{1}{N} \sum_{n=1}^N EE_i^n$$

$$\mu_i^* = \frac{1}{N} \sum_{n=1}^N |EE_i^n|$$

$$\sigma_i = \sqrt{\frac{1}{N} \sum_{n=1}^N (EE_i^n - \mu_i)^2}$$

The mean and modified mean give an indication of the overall effect of an input on the output. The standard deviation indicates the presence of nonlinear effects or interactions between the  $i^{\text{th}}$  parameter and the other parameters. Note that the modified mean is calculated because the EEs for a certain input may change sign on the output in case of non-monotonic functions, resulting in a cancellation effect. The mean, modified mean, and the standard deviations of a certain input can be inspected to get a qualitative measure of its significance. Larger  $\mu_i^*$  (or  $\mu_i$ ) values indicates the parameter is more important, while larger  $\sigma_i$  values mean the input parameter has a non-linear and/or interaction effect on the model output.

### 3 BISON Modeling

#### 3.1 UO<sub>2</sub> fuel and Cr<sub>2</sub>O<sub>3</sub>-doped UO<sub>2</sub> fuel in BISON

The initial average grain size for the doped fuel is modeled to be 56  $\mu\text{m}$ , which corresponds to 0.16 wt.% (i.e. 1600 ppm) of Cr<sub>2</sub>O<sub>3</sub> dopant in UO<sub>2</sub> [11]. The average grain size for standard UO<sub>2</sub> fuel is taken to be 15.6  $\mu\text{m}$  [12]. Fission gas behavior and release models from [13][14] are used in the BISON modeling for both the doped fuel and undoped fuel. For the doped fuel, the intra-granular diffusion coefficient from Turnbull et al. [15] is used, and a correction factor of three for the effective diffusion coefficient is adopted based on [3][16]. For the undoped fuel, the Andersson model [17] for the intra-granular diffusion coefficient is used. A modified Mikic-Todreas model [18] for solid-solid contact conductance is implemented into BISON and used in this work for both doped and undoped fuels. In this study we considered a standard nominal value for densification, while future work will aim to include the suppression in densification in Cr-doped fuel compared to standard UO<sub>2</sub>. The BISON setup used in this work for the Cr<sub>2</sub>O<sub>3</sub>-doped UO<sub>2</sub> fuel and standard UO<sub>2</sub> fuel has been validated against Halden experiments [19].

#### 3.2 LB-LOCA modeling in BISON

Large-break loss of coolant accident (LB-LOCA) is one of the most limiting scenarios for the fuel rods. Rapid loss of coolant leads to steep rise in fuel temperature and accelerated cladding oxidation. Cladding ballooning due to degradation in the cladding mechanical strength potentially leads to fuel rod rupture, after which the radioactive fission gases are released and contaminate the primary loop [20]. Reduced cladding ballooning in the Zr-4 cladding improves the resistance to burst failure as well as potential blockage in the coolant channel, providing longer survival time. Enhanced fission gas retention reduces the amount of released radioactive contamination upon fuel rod rupture. For these reasons, the LB-LOCA responses for both standard UO<sub>2</sub> fuel and Cr<sub>2</sub>O<sub>3</sub>-doped UO<sub>2</sub> fuel are modeled and compared in BISON. This work simulates a LB-LOCA in a prototypical PWR.

The traditional UO<sub>2</sub> and doped UO<sub>2</sub> fuel are first operated under normal operation, i.e. with linear heat generation rate (LHGR) of 21 kW/m with shutdown periods considered for ~636 days to a burnup of ~26 MWd/kgU. The LOCA scenario is pre-simulated using system code RELAP5 [21], and the LHGR, coolant pressure and cladding outer surface

temperature are prescribed in the BISON input using the RELAP5 results. Figure 1 presents the reactor power and coolant pressure vs. time upon the initiation of LOCA, and Figure 2 shows the cladding outer surface temperature during the LOCA progression as a function of the normalized fuel elevation. Chopped-cosine shape peaking factor with a peak-to-average ratio of  $\sim 1.5$  is used for both RELAP5 and BISON. In this work, the LOCA process is simulated until the fuel rods rupture. The maximum fuel temperature, plenum pressure, fission gas release, maximum oxide thickness and cladding ballooning size at the time of rupture, as well as the fuel survival time upon the start of LOCA, are taken as figure of merits (FOM) for the subsequent sensitivity study.

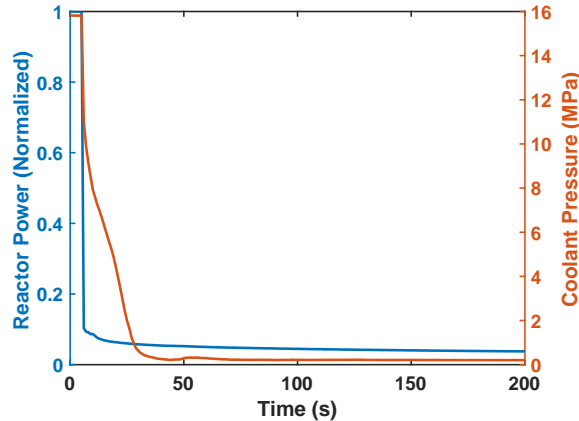


Figure 1. Normalized reactor power and coolant pressure vs. time during LOCA from the RELAP5 result (used as BISON input).

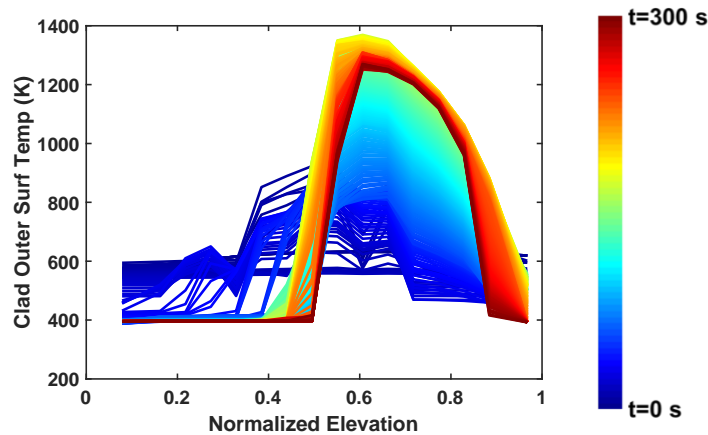


Figure 2. Progression of cladding outer surface temperature vs. normalized elevation during LOCA from the RELAP5 result (used as BISON input). Each curve corresponds to cladding outer surface temperature upon the initiation of LOCA until 300 seconds.

## 4 Sensitivity Analysis of LB-LOCA

### 4.1 BISON uncertainty input parameters

To conduct SA for the LB-LOCA case, a full list of uncertain parameters in BISON and their corresponding distributions and uncertain ranges have been identified. Table 1 shows the normally-distributed uncertain parameters with their mean values and standard deviations. All the normally-distributed uncertain parameters are truncated to

$\pm 2\sigma$  range (95% confidence interval) in the sampling process. Table 2 lists all the uniformly-distributed uncertain parameters and their corresponding uncertain ranges, and Table 3 shows the uncertain parameters in the FGR model with log-normal distribution. Most of the parameter uncertainties are obtained based on expert opinion from previous research [22-30]. The last columns of Table 1-3 include the sources of such information. Uncertainties for inputs that cannot be found or have never been considered previously are defined based on the authors' own evaluation, for example, cladding hardening modulus, fuel solid swelling and gaseous swelling. MOAT is used for SA with DAKOTA code [9], and 2250 sampling are used for both  $UO_2$  and doped fuel.

Label	Descriptor	Description	Properties*	Mean	Standard Deviation
x1	clad_thickness	Cladding thickness	A	6.1e-4 m	1.85% [22]
x2	pellet_outer_radius	Pellet outer radius	A	0.00413 m	0.05% [22]
x3	grain_radius	Fuel grain radius	A	7.8e-6 m (undoped)	30% [23]
				28e-6 m (doped)	30% [23]
x4	power_scalef	LHGR	M	1.0	1% [24][25]
x5	coolant_inlet_pressure_scalef	Coolant inlet pressure	M	1.0	1% [26]
x6	roughness_fuel	Fuel outer surface roughness	A	2e-6 m	12.5% [24]
x7	roughness_clad	Cladding inner surface roughness	A	1e-6 m	15% [24]
x8	NFIR_const_scalef	Constant term within the phonon contribution in NFIR model	M	1.0	25% [27]
x9	NFIR_bu_scalef1	The burnup-dependent term in the phonon contribution at the start of thermal recovery in NFIR model	M	1.0	6% [27]
x10	NFIR_bu_scalef2	The burnup-dependent term in the phonon contribution at the end of thermal recovery in NFIR model	M	1.0	6% [27]
x11	thermal_expansion_fuel	Fuel thermal expansion	A	10e-6	7.5% [22][25]
x12	thermal_expansion_clad	Clad thermal expansion	A	5e-6	15% [22]
x13	clad_irradiation_creep_scalef	Clad irradiation creep	M	1.0	11% [28]
x14	clad_thermal_creep_scalef	Clad thermal creep	M	1.0	14.5% [28]
x15	clad_loca_creep_scalef	Clad thermal creep during LOCA	M	1.0	14.5% [28]
x16	hardening_scalef	Clad hardening modulus	M	1.0	10%
x17	fuel_solid_swell_scalef	Fuel solid swelling	M	1.0	10%
x18	fuel_gas_swell_scalef	Fuel gaseous swelling	M	1.0	20%
x19	fuel_temperature_scalef	Fuel temperature in FGR model	M	1.0	2.5% [23]
x20	oxidation_scalef	Oxidation thickness	M	1.0	20% [22][25]
x21	emissivity_fuel	Fuel emissivity	A	0.87	3% [29]

Table 1. Normally distributed BISON uncertain parameters.

\*In the "Properties" column, "A" denotes "Additive", and "M" refers to "Multiplicative"

Label	Descriptor	Description	Properties*	Nominal	Range
x22	pellet_height	Pellet height	A	0.10 m	±0.5% [26]
x23	clad_top_gap_height	Plenum length	A	5.08552e-3 m	±0.5% [26]
x24	clad_gap_width	Gap size	A	7.5e-5 m	±2.5% [26]
x25	fast_neutron_flux_normal_scalef	Fast neutron flux during normal operation	M	3e13	±5% [26]
x26	fast_neutron_flux_loca_scalef	Fast neutron flux during LOCA	M	0.16e15	±5% [26]
x27	u235_enrich	<sup>235</sup> U enrichment	A	0.0293	±0.25% [26]
x28	emissivity_clad	Clad emissivity	A	0.25	±5% [26][30]
x29	gascond_scalef	Gas conductance	M	1.0	±10% [26]
x30	contactcond_scalef	Solid-solid contact conductance	M	1.0	±50% [26]
x31	cp_scalef	Fuel specific heat	A	1.0	±5% [26]
x32	youngs_modulus_fuel	Fuel Young's modulus	A	2.0e11 Pa	±5% [26]
x33	poissons_ratio_fuel	Fuel Poisson's ratio	A	0.345	±17.5% [26]
x34	fuel_creepstrain_scalef	Fuel creep strain	M	1.0	±10% [26]
x35	relocation_scalef	Fuel relocation strain	M	1.0	±5% [26]
x36	thermal_conductivity_clad	Clad thermal conductivity	A	16 W/(m K)	±2.5% [26]
x37	specific_heat_clad	Clad specific heat	A	330 J/(kg K)	±2.5% [26]
x38	youngs_modulus_clad	Clad Young's modulus	A	7.5e10 Pa	±2.5% [26]
x39	poissons_ratio_clad	Clad Poisson's ratio	A	0.3	±2.5% [26]
x40	fuel_densification	Fuel densification	A	0.01	±0.5% [26]
x41	clad_outer_surface_temp_uncertainty	Clad outer surface temperature	A	-	±3K [26]

Table 2. Uniformly distributed BISON uncertain parameters.

\*In the "Properties" column, "A" denotes "Additive", and "M" refers to "Multiplicative"

Label	Descriptor	Description	Properties*	Nominal	Range
x42	igdiffcoeff_scalef	Intra-granular atomic diffusion coefficient	M	1.0	Factor of 100 [23]
x43	resolutionp_scalef	Intra-granular resolution parameter	M	1.0	Factor of 100 [23]
x44	gbdiffcoeff_scalef	Grain-boundary diffusion coefficient	M	1.0	Factor of 100 [23]

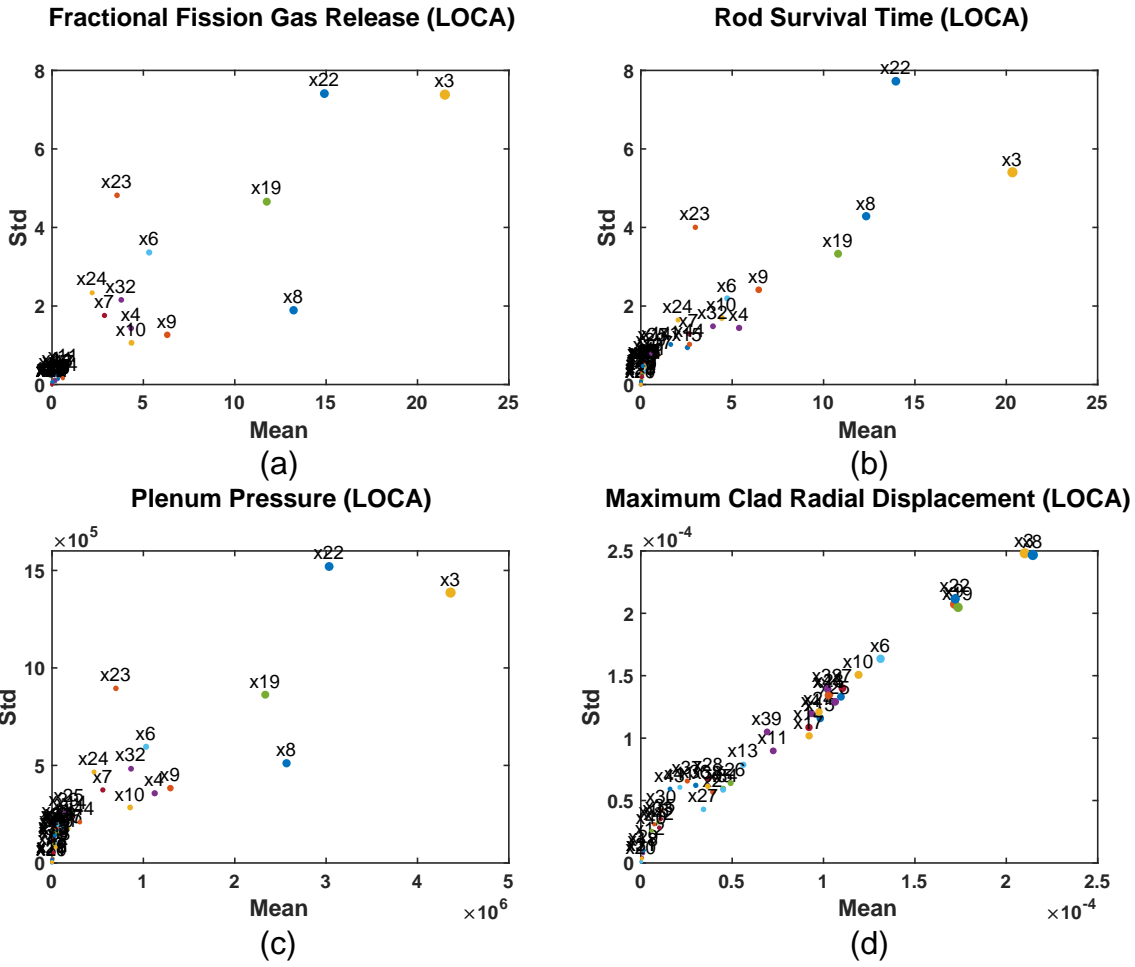
Table 3. Log-normally distributed BISON uncertain parameters.

\*In the "Properties" column, "A" denotes "Additive", and "M" refers to "Multiplicative"

## 4.2 SA results using MOAT

Figure 3 presents two sensitivity measures for the standard UO<sub>2</sub> fuel: mean values and standard deviations of the EEs for each input parameter with respect to six selected response functions: (a) fractional fission gas release, (b) rod survival time, (c) plenum pressure, (d) maximum cladding radial displacement, (e) maximum oxide thickness and (f) maximum fuel temperature at the end of LB-LOCA when the clad bursts. Figure 4 shows the same sensitivity measurements for Cr<sub>2</sub>O<sub>3</sub>-doped UO<sub>2</sub> fuel. The mean values

are estimation of the overall influence of each uncertain input to the response function, and the importance of the uncertain parameters are ranked in order of the mean value [31]. A parameter is considered to be “important” if its mean value exceeds 20% of the largest mean value among all the 44 inputs for at least one of the six response functions. Table 4 shows the filtered important uncertain parameters for both standard UO<sub>2</sub> fuel and Cr<sub>2</sub>O<sub>3</sub>-doped UO<sub>2</sub> fuel. 25 of the 44 inputs are considered to be non-negligible. The standard deviations measure the non-linearity and/or interactions with other parameters and will be used to gain more insights in the future work.



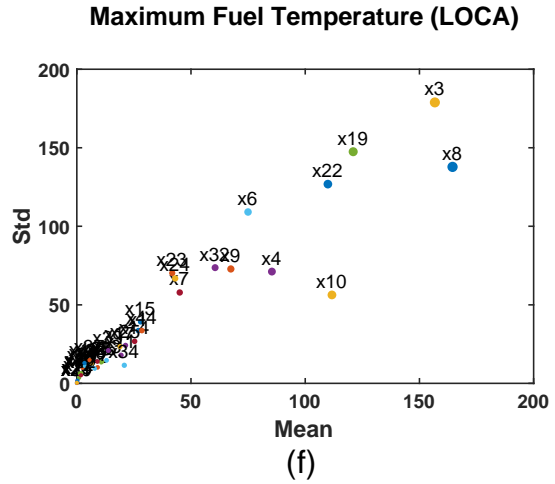
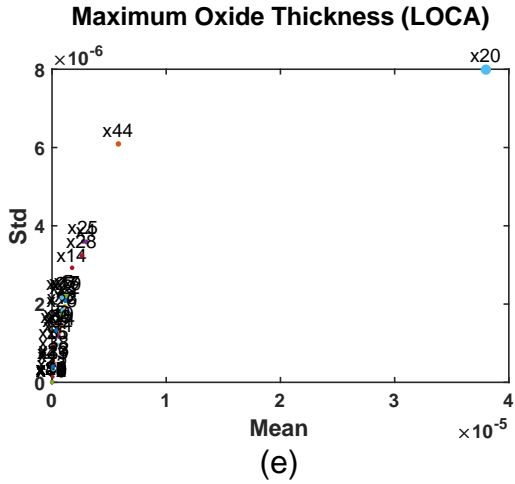
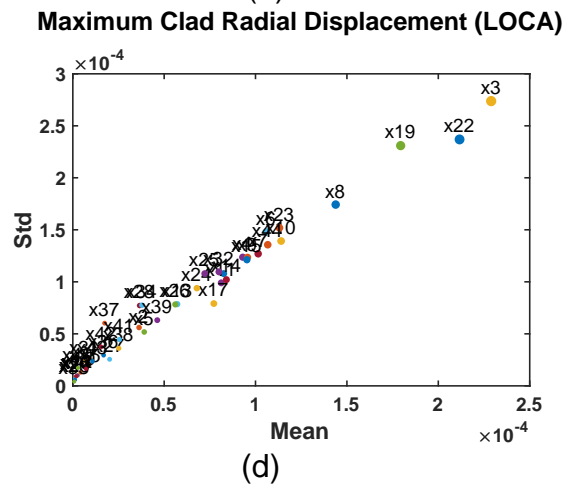
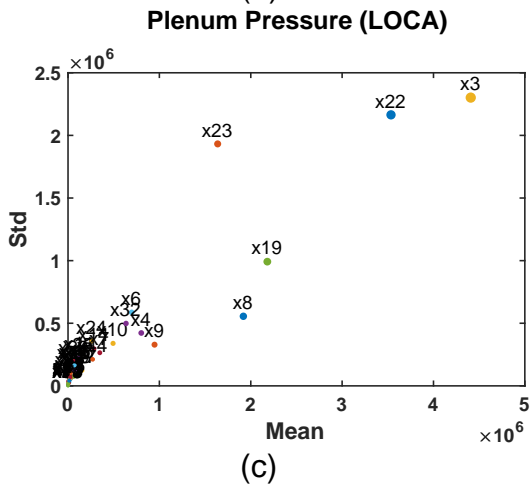
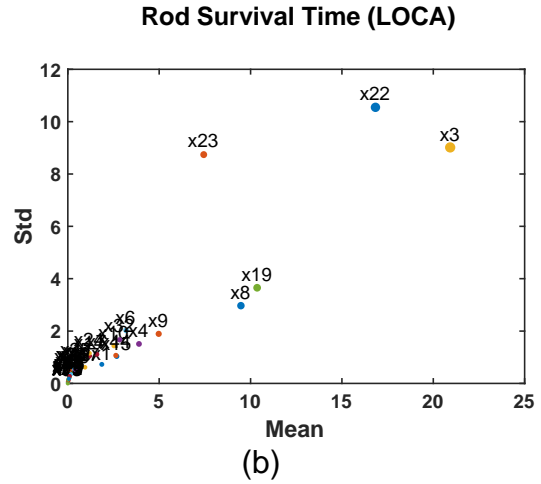
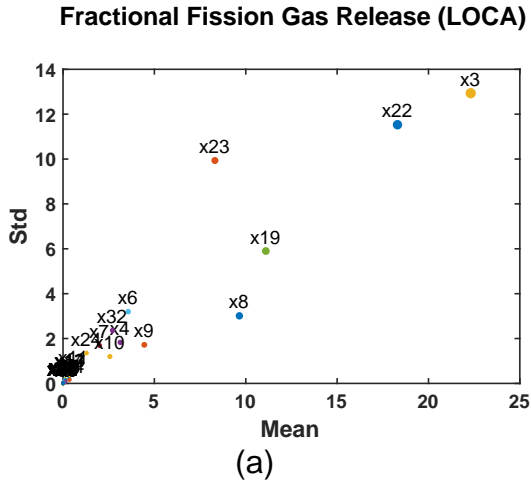


Figure 3. Standard deviation vs. mean value for the response functions in the Morris Screening result for standard UO<sub>2</sub> fuel.





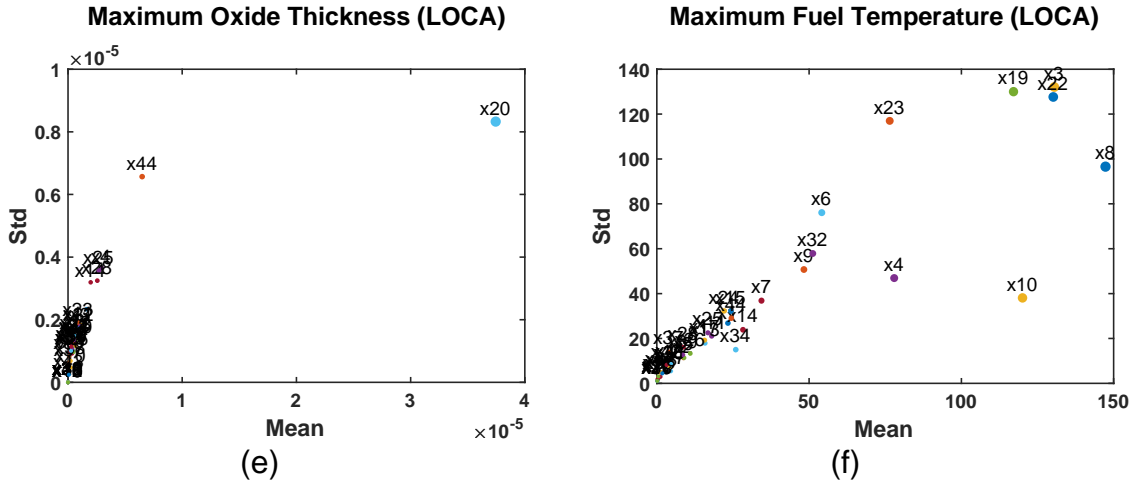


Figure 4. Standard deviation vs. mean value for the response functions in the Morris Screening result for  $\text{Cr}_2\text{O}_3$ -doped  $\text{UO}_2$  fuel.

Category	Label	Descriptor	Property
Manufacturing	x1	clad_thickness	Geometry
	x6	roughness_fuel	Manufacturing
	x7	roughness_clad	Manufacturing
	x21	pellet_height	Geometry
	x22	clad_top_gap_height	Geometry
Fuel Model Properties	x23	clad_gap_width	Geometry
	x8	NFIR_const_scalef	Fuel thermal conductivity
	x9	NFIR_bu_scalef1	Fuel thermal conductivity
	x10	NFIR_bu_scalef2	Fuel thermal conductivity
	x11	thermal_expansion_fuel	Fuel thermal expansion
	x17	fuel_solid_swell_scalef	Fuel solid swelling
Fission Gas Release Model	x32	youngs_modulus_fuel	Fuel mechanical property
	x34	fuel_creepstrain_scalef	Fuel creep
	x3	grain_radius	FGR model
	x19	fuel_temperature_scalef	FGR model
Clad Model Properties	x44	gbdiffcoeff_scalef	FGR model
	x13	clad_irradiation_creep_scalef	Clad irradiation creep
	x14	clad_thermal_creep_scalef	Clad thermal creep
	x15	clad_loca_creep_scalef	Clad thermal creep in LOCA
	x20	oxidation_scalef	Clad oxidation
Operating Conditions	x39	poissons_ratio_clad	Clad mechanistic model
	x4	power_scalef	Power history
	x5	coolant_inlet_pressure_scalef	Coolant inlet pressure
	x24	fast_neutron_flux_normal_scalef	Fast neutron flux
	x25	fast_neutron_flux_loca_scalef	Fast neutron flux

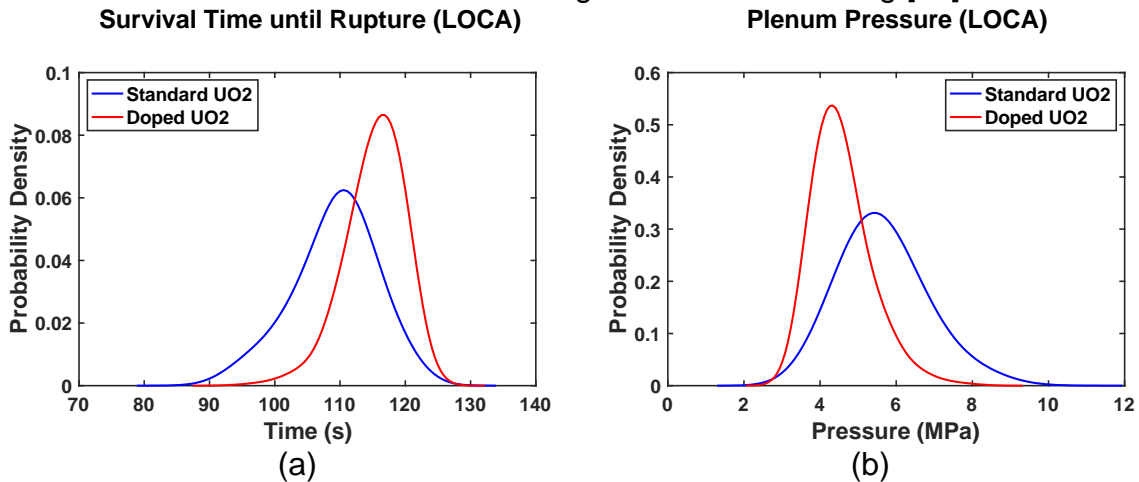
Table 4. Filtered uncertain input parameters based on the importance (mean value) using a cutoff value of 20%.

Note that the screening process only provides qualitative measures. The MOAT results in Figures 4-5 can only be used to rank the importance of the uncertain inputs. They contain no information about how the input uncertainties contribute to each of the responses. In other words, MOAT can be used to identify the non-influential inputs but cannot accurately quantify the contributions of the influential inputs. Advanced SA methods such as variance based decomposition can be used to provide such quantitative measures. MOAT is useful in the early phase a SA to identify the non-influential input parameters and reduce the input dimension for subsequent analysis.

## 5 Uncertainty Quantification of LB-LOCA

UQ is subsequently performed for both standard  $\text{UO}_2$  fuel and  $\text{Cr}_2\text{O}_3$ -doped  $\text{UO}_2$  fuel based on the SA results from the previous section. Only parameters that are considered non-trivial on the selected FOMs are used during UQ. Latin Hypercube Sampling (LHS) is used to propagate the uncertainties from the selected inputs to the FOMs, and 2000 samples are used.

Figure 5 shows the probability density functions (PDFs) for the six selected response functions. It is shown that  $\text{Cr}_2\text{O}_3$ -doped  $\text{UO}_2$  fuel has a greater probability to survive longer before burst than the standard  $\text{UO}_2$  fuel during LOCA. When the fuel rod fails, the plenum pressure within the doped fuel is lower than the standard  $\text{UO}_2$  fuel due to less release of gaseous fission products. The maximum oxide thickness until the fuel rod rupture does not show much difference due to the fixed cladding outer surface temperature used in the simulation. The maximum fuel temperature in the doped fuel is lower than the standard  $\text{UO}_2$  fuel. This is because in the doped fuel less fission gas is released into the gap, hence the gap conductance deteriorates less compared to the undoped fuel. Finally, the cladding radial displacement with respect to the cladding elevation is shown in Figure 6. The ballooning effect in the doped fuel is slightly less severe compared to the standard  $\text{UO}_2$  fuel, and it is subject to less uncertainty. Standard deviations are shown in Table 5, which shows that the standard deviations are mostly comparable. Among all the response functions, fission gas release and plenum pressure are subject to the largest uncertainty, which confirms the conclusions of previous studies on uncertainties in fission gas behavior modeling [23].



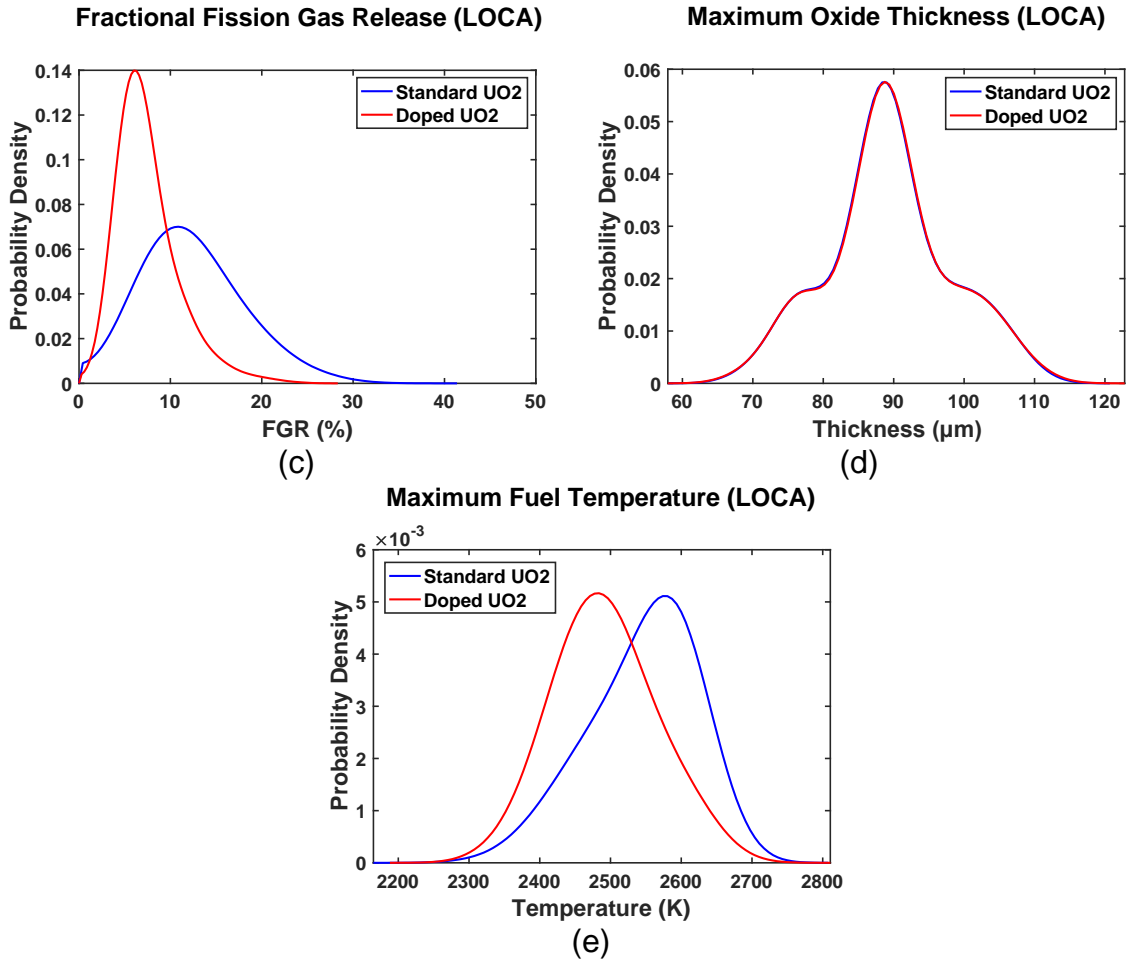


Figure 5. Comparison of PDFs of five FOMs for standard UO<sub>2</sub> fuel and Cr<sub>2</sub>O<sub>3</sub>-doped UO<sub>2</sub> fuel.

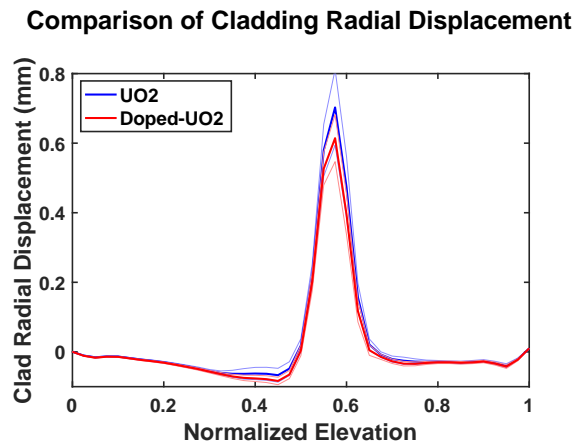


Figure 6. Comparison of cladding radial displacement with respect to normalized elevation upon rod rupture for standard UO<sub>2</sub> fuel and Cr<sub>2</sub>O<sub>3</sub>-doped UO<sub>2</sub> fuel. Solid lines denote the mean value and the error bands show ±σ range.

Response functions	UO <sub>2</sub>	Cr <sub>2</sub> O <sub>3</sub> -doped UO <sub>2</sub>
--------------------	-----------------	---

Rod survival time during LOCA	6.1	4.3
Plenum pressure	1.1	0.7
Fractional fission gas release (%)	5.12	3.25
Maximum oxide thickness ( $\mu\text{m}$ )	8.50	8.58
Maximum fuel temperature (K)	71.1	67.9
Maximum cladding radial displacement (mm)	0.108	0.068

Table 5. Standard deviation ( $\pm\sigma$ ) for the six response functions.

## 6 Conclusions

This work showed a sensitivity and uncertainty analysis of fuel performance modeling during a large-break LOCA for standard and Cr<sub>2</sub>O<sub>3</sub>-doped UO<sub>2</sub> fuels, using the BISON code. Morris screening was used to identify the non-influential uncertainty input parameters, and the FOM uncertainties for both fuels are quantified based on the selected parameters from the SA results. It was shown that Cr<sub>2</sub>O<sub>3</sub>-doped UO<sub>2</sub> fuel provides longer survival upon LB-LOCA compared to the standard UO<sub>2</sub> fuel and slight less severe cladding ballooning upon the fuel rod failure. Upon the rod rupture, less radioactive nuclides would be released into the primary loop in the doped fuel case, due to a lower amount of released fission gas throughout the life. Less released gaseous fission products also correspond to less contaminants into the gap, providing slightly lower maximum fuel temperature. Because of these characteristics, our calculations therefore indicate that Cr<sub>2</sub>O<sub>3</sub>-doped UO<sub>2</sub> fuel provides enhanced accident tolerance for LB-LOCA scenarios compared to standard UO<sub>2</sub> fuel. The enhanced PCMI in the doped fuel, as well as the parameter interaction in the Morris method will be used to gain more insight in benefits of doped UO<sub>2</sub> fuel in future work.

## References

- [1]. Zinkle, S. J., Terrani, K. A., Gehin, J. C., Ott, L. J., & Snead, L. L. (2014). Accident tolerant fuels for LWRs: A perspective. *Journal of Nuclear Materials*, 448(1-3), 374-379.
- [2]. Bourgeois, L., Dehaut, P., Lemaignan, C., & Hammou, A. (2001). Factors governing microstructure development of Cr<sub>2</sub>O<sub>3</sub>-doped UO<sub>2</sub> during sintering. *Journal of nuclear materials*, 297(3), 313-326.
- [3]. Killeen, J. C. (1980). Fission gas release and swelling in UO<sub>2</sub> doped with Cr<sub>2</sub>O<sub>3</sub>. *Journal of Nuclear Materials*, 88(2-3), 177-184.
- [4]. Lysikov, A. V., Mikheev, E. N., Novikov, V. V., & Pimenov, Y. V. (2010). High Burnup UO<sub>2</sub> Fuel Pellets with Dopants for WWER. *Advanced Fuel Pellet Materials and Fuel Rod Design for Water Cooled Reactors*, 107.
- [5]. Massih, A. (2014). Effects of additives on uranium dioxide fuel behavior.
- [6]. Topical Report, "Incorporation of Chromia-Doped Fuel Properties in AREVA Approved Methods," AREVA Inc., ANP-10340NP, Revision 0, 2016.
- [7]. Langewisch, D. R. (2010). *Uncertainty and sensitivity analysis for long-running computer codes: a critical review* (Doctoral dissertation, Massachusetts Institute of Technology).
- [8]. Williamson, R. L., Hales, J. D., Novascone, S. R., Tonks, M. R., Gaston, D. R., Permann, C. J., ... & Martineau, R. C. (2012). Multidimensional multiphysics simulation of nuclear fuel behavior. *Journal of Nuclear Materials*, 423(1-3), 149-163.
- [9]. Adams, B. M., et al. (2018). Dakota, a multilevel parallel object-oriented framework for design optimization, parameter estimation, uncertainty quantification, and sensitivity analysis: Version 6.8 user's manual. Technical report, Sandia National Laboratories, Tech. Rep. SAND2014-4633, Updated May 8, 2018.
- [10]. Morris, M. D. (1991). Factorial sampling plans for preliminary computational experiments. *Technometrics*, 33(2), 161-174.

- [11]. C. Delafoay et al., (2015) "AREVA Cr<sub>2</sub>O<sub>3</sub>-doped fuel: Increase in operational flexibility and licensing margins" in proceedings of Top Fuel 2015, Reactor Fuel Performance Meeting. Zurich, Switzerland. Sept. 13-17.
- [12]. Josek, R. (2008). The high initial rating test IFA-677.1: Final report on in-pile results. *Technical Report HWR-872, Institutt for Energiteknik, Halden, Norway.*
- [13]. Pastore, G., Luzzi, L., Di Marcello, V., & Van Uffelen, P. (2013). Physics-based modelling of fission gas swelling and release in UO<sub>2</sub> applied to integral fuel rod analysis. *Nuclear Engineering and Design, 256*, 75-86.
- [14]. Barani, T., Bruschi, E., Pizzocri, D., Pastore, G., Van Uffelen, P., Williamson, R. L., & Luzzi, L. (2017). Analysis of transient fission gas behaviour in oxide fuel using BISON and TRANSURANUS. *Journal of Nuclear Materials, 486*, 96-110.
- [15]. Turnbull, J. A., Friskney, C. A., Findlay, J. R., Johnson, F. A., & Walter, A. J. (1982). The diffusion coefficients of gaseous and volatile species during the irradiation of uranium dioxide. *Journal of Nuclear Materials, 107(2-3)*, 168-184.
- [16]. Kashibe, S., & Une, K. (1998). Effect of additives (Cr<sub>2</sub>O<sub>3</sub>, Al<sub>2</sub>O<sub>3</sub>, SiO<sub>2</sub>, MgO) on diffusional release of <sup>133</sup>Xe from UO<sub>2</sub> fuels. *Journal of nuclear materials, 254(2-3)*, 234-242.
- [17]. Andersson, D. A., Garcia, P., Liu, X. Y., Pastore, G., Tonks, M., Millett, P., ... & Martineau, R. C. (2014). Atomistic modeling of intrinsic and radiation-enhanced fission gas (Xe) diffusion in UO<sub>2</sub>±x: Implications for nuclear fuel performance modeling. *Journal of Nuclear Materials, 451(1-3)*, 225-242.
- [18]. Jacobs, G., & Todreas, N. (1973). Thermal contact conductance in reactor fuel elements. *Nuclear science and engineering, 50(3)*, 283-290.
- [19]. (Accepted) Che, Y., Pastore, G., Hales, J., & Shirvan, K., "Modeling of Cr<sub>2</sub>O<sub>3</sub>-doped UO<sub>2</sub> as a Near-term Accident Tolerant Fuel for LWRs using the BISON Code," Nuclear Engineering and Design, 2018.
- [20]. Perez, D. M., Williamson, R. L., Novascone, S. R., Pastore, G., Hales, J., & Spencer, B. W. (2013). Assessment of BISON: A nuclear fuel performance analysis code. *Idaho National Laboratory, Idaho Falls.*
- [21]. Feng, D., Hejzlar, P., & Kazimi, M. S. (2007). Thermal-hydraulic design of high-power-density annular fuel in PWRs. *Nuclear Technology, 160(1)*, 16-44.
- [22]. Ikonen, T., & Tulkki, V. (2014). The importance of input interactions in the uncertainty and sensitivity analysis of nuclear fuel behavior. *Nuclear Engineering and Design, 275*, 229-241.
- [23]. Pastore, G., Swiler, L. P., Hales, J. D., Novascone, S. R., Perez, D. M., Spencer, B. W., ... & Williamson, R. L. (2015). Uncertainty and sensitivity analysis of fission gas behavior in engineering-scale fuel modeling. *Journal of Nuclear Materials, 456*, 398-408.
- [24]. Lee, J., & Woo, S. (2014). Effects of fuel rod uncertainty on the LBLOCA safety analysis with limiting fuel burnup change. *Nuclear Engineering and Design, 273*, 367-375.
- [25]. Blakely, C., Zhang, H., & Ban, H. (2018). Sensitivity analysis of VERA-CS and FRAPCON coupling in a multiphysics environment. *Annals of Nuclear Energy, 111*, 683-701.
- [26]. Unal, C., Williams, B. J., Yacout, A., & Higdon, D. M. (2013). Application of advanced validation concepts to oxide fuel performance codes: LIFE-4 fast-reactor and FRAPCON thermal-reactor fuel performance codes. *Nuclear Engineering and Design, 263*, 102-128.
- [27]. Bouloré, A., Struzik, C., & Gaudier, F. (2012). Uncertainty and sensitivity analysis of the nuclear fuel thermal behavior. *Nuclear Engineering and Design, 253*, 200-210.
- [28]. Geelhood, K. J., Luscher, W. G., Raynaud, P., & Porter, I. (2011). FRAPCON-4.0: A Computer Code for the Calculation of Steady-State. *Thermal-Mechanical Behavior of Oxide Fuel Rods for High Burnup (NUREG/CR-7022, Volume 1, PNNL-19418, Volume 1), published March.*
- [29]. Lee, P. Y. (1993). *Thermophysical property measurements at high temperatures for liquid metal alloys and gadolinium oxide-doped uranium dioxide samples* (Doctoral dissertation, Rice University).
- [30]. Mathew, P. M., & George, I. M. (1996). Total emissivity of Zircaloy-4 at high temperatures. In *17th Annual Canadian Nuclear Society Conference.*
- [31]. Kristensen, M. H., & Petersen, S. (2016). Choosing the appropriate sensitivity analysis method for building energy model-based investigations. *Energy and Buildings, 130*, 166-176.